TABLE IV. Charge per nucleon of the fissioning nucleus and of its average light and heavy fission fragments. In the computation of the data based on Table II, U^{236} was used as the reference nuclide.

Compound nucleus	$Z/(Z+N)$	$\bar{Z}_L/(\bar{Z}_L+\bar{N}_H)$ from: Eqs. (5)	Table II	$\bar{Z}_H/(\bar{Z}_L+\bar{N}_H)$ from: Eqs. (5)	Table II
Th^{233}	0.389	0.399	0.400	0.386	0.385
U^{234}	0.395	0.406	0.405	0.392	0.393
U^{236}	0.394	0.402	0.402	0.389	0.389
U^{238}	0.390	0.399	0.399	0.385	0.386
U^{239}	0.389	0.397	0.398	0.384	0.383
Pu^{240}	0.396	0.404	0.402	0.390	0.391
Cm^{242}	0.401	0.408	0.405	0.390	0.392
Cf^{252}	0.393	0.399	0.399	0.385	0.388
Average	0.393	0.402	0.401	0.387	0.388

The average charge of the heavy fragment is almost independent of the neutron contents, indicating a high selectivity with respect to charge, associated with an indifference with respect to neutron contents.

(2) $\bar{Z}$ *versus* $\bar{A}$: A very regular relationship exists between $\bar{Z}$ and $\bar{A}$ for both the light and the heavy fragment. As Table IV shows, the ratio Z/A, which may be called the charge density, or charge per nucleon, has a constant value for each group of fragments, regardless of the nature of the fissioning nucleus. The mean value of the constant is 0.402 for the light fragment and 0.387 for the heavy fragment. In all cases the charge density of the fissile nucleus is larger than the charge density of the heavy fragment and smaller than that of the light fragment, giving no support to the "unchanged charge ratio" postulate,[9] also in cases other than that of the thermal neutron fission of U^{235}.

The relationship between the average charge and mass of the light and heavy fragments leads to two almost parallel straight lines (Fig. 2), which almost coincide with the Z_p versus A lines for $U^{235}(n,F)$, implying that the relationship between the most probable values of fragment charge and mass is independent of the fissioning nucleus; in other words, this relationship is *universal.*

The average charge and mass of the light fragment vary within much wider limits (8 charge units and 18 mass units, respectively), in comparison to the heavy fragment charge and mass which vary in a much narrower range (2 charge units and 6 mass units, respectively), signifying that the fission process is more selective with respect to the heavy-fragment composition.

[9] N. Sugarman and A. Turkevich, private communication to Professor Coryell; C. D. Coryell, M. Kaplan, and R. D. Fink, Can. J. Chem. **39**, 646 (1961).

PHYSICAL REVIEW VOLUME 134, NUMBER 5B 8 JUNE 1964

(d,He^3) Reaction on Ca^{40} and the Titanium Isotopes*

J. L. YNTEMA
Argonne National Laboratory, Argonne, Illinois
AND
G. R. SATCHLER
Oak Ridge National Laboratory, Oak Ridge, Tennessee

(Received 31 January 1964)

The (d,He^3) reaction on Ca^{40} and isotopically enriched targets of Ti^{46}, Ti^{47}, Ti^{48}, Ti^{49}, and Ti^{50} has been investigated. Absolute differential cross sections for a number of transitions were obtained over an angular range from 11 to 33°. The angular distributions are compared with distorted-wave calculations which use the optical-model-potential parameters derived from the elastic scattering of 21-MeV deuterons on the same target materials. The data for the elastic scattering are given together with the optical-model fits. The $Ca^{40}(d,He^3)K^{39}$ reaction was used to obtain the normalization coefficients necessary to extract spectroscopic factors from the comparison of the measured and calculated differential cross sections. The results show that the excitation energies of the $d_{3/2}$ and $s_{1/2}$ proton-hole states are surprisingly low and increase with the number of $f_{7/2}$ neutrons in the nucleus. In the case of Sc^{45}, the $d_{3/2}$ hole state which contains the full $d_{3/2}$ strength is found at an excitation energy of less than 50 keV. The excitation energy of the $d_{3/2}$ hole state increases to 800 keV for Sc^{47} and to about 2.4 MeV in Sc^{49}. The excitation energy of the $s_{1/2}$ hole state increases from 0.92 MeV in Sc^{45} to 2.1 MeV in Sc^{48}.

1. INTRODUCTION

IN recent years a number of papers have reported experiments on reactions in which a neutron from the target nucleus is captured by the bombarding nucleus. These experiments have been used in particular to obtain information on the ground-state wave functions of the target nucleus and, in some cases, on the final nucleus. Only a small number of experiments on reactions involving the capture of a proton from the target nucleus have been reported.[1-3] It has been

* Work performed under the auspices of the U. S. Atomic Energy Commission.

[1] J. L. Yntema, T. H. Braid, B. Zeidman, and H. W. Broek, in *Proceedings of the Rutherford Jubilee International Conference,*

shown that in the (d,He^3) reaction[1] the angular distribution of the outgoing particle can be used to indicate the orbital angular momentum of the captured proton. In the case of the $V^{51}(n,d)Ti^{50}$ reaction, the experimental angular distribution has been compared in considerable detail with the angular distribution obtained from distorted-wave calculations.

The present experiment primarily concerns the Ti(d,He^3)Sc reactions on enriched targets of the five stable Ti isotopes. According to the simple shell model, the Ti isotopes have two $1f_{7/2}$ protons and from four to eight $1f_{7/2}$ neutrons outside of the closed sd-shell core. The experiment may therefore provide information on the excitation energies of the d and s hole states in the scandium isotopes and also to some extent on the possibility of excited-core proton configurations in the ground-state wave functions of the titanium isotopes. Furthermore, the large negative Q values which occur even for the ground-state transitions allow one to obtain some information on how the angular distribution for a given value of l depends on the Q value of the transition.

2. EXPERIMENTAL PROCEDURE

The experiment was done with the 21.5-MeV deuteron beam from the Argonne 60-in. cyclotron. The targets were mounted in the foil changer of the 60-in. scattering chamber.[4] The detection unit consisted of an $E-dE/dx$ telescope in which both the dE/dx and E detectors were surface-barrier silicon diodes. Since in nearly all cases Q is very negative, the energy of the He^3 particles is rather low. Consequently, the target thickness contributes considerably to the linewidth. In order to avoid additional loss of resolution because of the thickness of the dE/dx detector, the signals of the dE/dx detector and E detector were added at the output of the preamplifiers. Although the adding circuitry indeed introduces some additional noise, this procedure nevertheless improved the resolution—reducing the linewidth from about 700 keV to about 350 keV.

The detector unit had a defined aperture with a diameter of 1.52 mm and was placed at a distance of 18 cm from the center of scattering. The current was integrated by means of the system of Ramler, Brookshier, and Benaroya.[5] The target thickness was measured by measuring the weight per unit area. In this particular case, since the material was not very malleable, this could lead to errors. However, the measurements on the elastic scattering of 21.5-MeV deuterons appear to indicate that the error does not exceed 5%.

The titanium foils were taken from the batch of material that was analyzed previously by the mass spectroscopy group of the Argonne Special Materials Division. The tabulated results of this analysis have already been published.[6] Contributions from isotopes other than the one with the highest concentration must be subtracted from the spectrum of He^3 particles from the main isotope. If an isotope makes a particularly strong contribution, its effect must be subtracted even if its concentration is only a few percent. The correction was made electronically by means of the "subtract" mode of the 400-channel analyzer. The spectrum of the primary sample was first accumulated until a given integrated charge had been received by the target. The contribution of each isotopic contaminant was then subtracted by inserting a target with that isotope as its main component and operating the analyzer in the "subtract" mode until the integrated charge reached a value determined by the thickness (mg/cm^2) of the target and the abundance of that contaminant isotope in the primary sample. The result was a satisfactory approximation to the spectrum of the pure isotope. It is quite clear that such a correction is not perfect and introduces slight shifts in peak positions, undercorrects the contaminating isotopes, and subtracts out some of the contributions from the isotope under consideration. However, such errors ordinarily are only a small fraction of the initial correction; the final accuracy did not warrant the use of a computer program for the reduction of the raw data to obtain the contributions of the individual isotopes.

The separation of the He^3 component of the reaction products was such that at least 90% of the He^3 particles were accepted.

In order to obtain an empirical result for the angular distributions corresponding to d-wave and s-wave proton pickup, a measurement was performed on a calcium target. The thickness of the target was determined by means of chemical analysis after the experiment in order to avoid uncertainties due to oxygen and hydrogen contamination in the target.

Data were obtained at angles from 12 to 30° in 3° steps; and in the case of Ti^{48}, also at 35 and 40°. This range should permit the identification of $l=0$, $l=1$, $l=2$, and $l=3$, and also permit the unraveling of cases in which more than one value of l is involved. For some isotopes, data were obtained also in the region between 30 and 52°. From an inspection of the unreduced data, it was clear that little or no additional information could be extracted. These data have not been included in the present analysis.

The energy calibration was obtained from the α-particle beam of the cyclotron. The energy of the cyclotron beam was measured with a system of absorber foils by use of the range-energy relation for α particles in Al. This calibration was in excellent agree-

Manchester, 1961 (Heywood and Company, Ltd., London, 1961), p. 521.

[2] Bibijana Čujec, Phys. Rev. **128**, 2303 (1962).

[3] K. Ilakovac, L. G. Kuo, M. Petravić, I. Šlaus, P. Thomaš, and G. R. Satchler, Phys. Rev. **128**, 2739 (1962).

[4] J. L. Yntema and H. W. Ostrander, Nucl. Instr. Methods **16**, 69 (1962).

[5] W. Ramler, R. Benaroya, and W. Brookshier (private communication).

[6] J. L. Yntema, Phys. Rev. **127**, 1659 (1962).

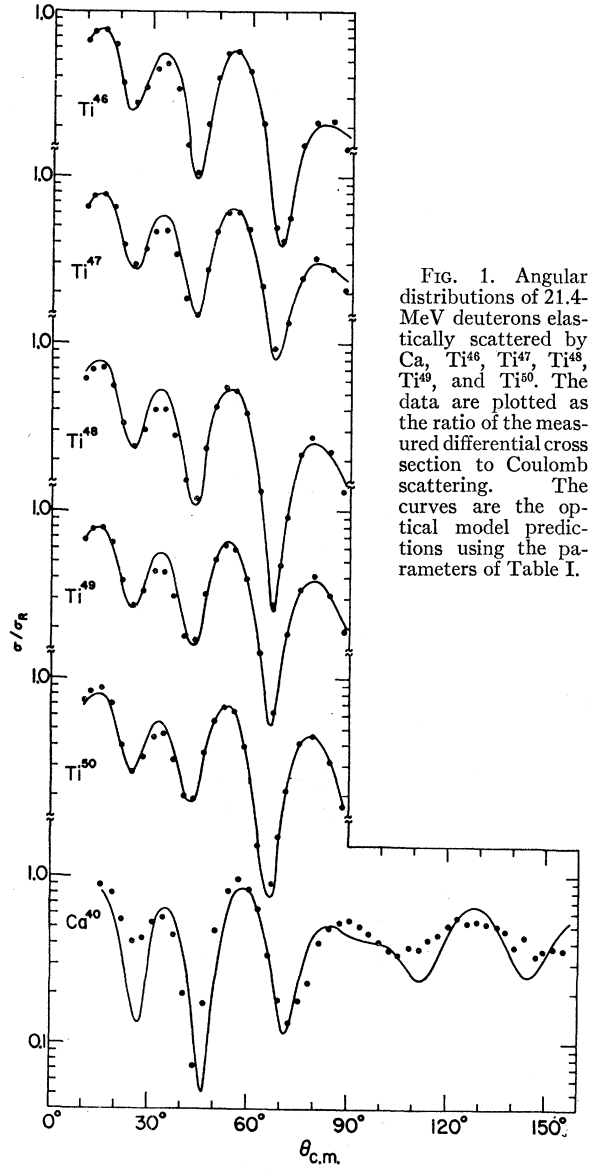

FIG. 1. Angular distributions of 21.4-MeV deuterons elastically scattered by Ca, Ti^{46}, Ti^{47}, Ti^{48}, Ti^{49}, and Ti^{50}. The data are plotted as the ratio of the measured differential cross section to Coulomb scattering. The curves are the optical model predictions using the parameters of Table I.

ment with the results from the $Ca^{40}(d,He^3)K^3$, and the $Ti^{48}(d,He^3)Sc^{47}$ ground-state transitions. Some uncertainty in the energy scale for low-energy He^3 particles is introduced by noise and the target thickness as well as by fluctuations in the incident-deuteron energy. Subsequently, an experiment was performed on very thin (≈ 0.3 mg/cm^2) targets. The energy calibration was obtained from a number of transitions with known Q values. The excitation energies given in this paper have been derived from these spectra.

3. DISTORTED-WAVE THEORY

The distorted-wave theory of nuclear direct reactions has been described in detail elsewhere.[7,8] For its application, one needs to know the optical-model parameters that describe the elastic scattering in the entrance and exit channels. For the reactions studied here, the elastic scattering of 21-MeV deuterons by both Ca^{40} and the Ti isotopes has been measured and analyzed. The optical-model fits are compared with experiment in Fig. 1, and the corresponding parameters are listed in Table I. The potential used was of the form

$$U(r)=-\frac{V+iW}{e^x+1}+4iW_D\frac{d}{dx'}\left(\frac{1}{e^x+1}\right)+V_c(r),$$

where $x=(r-r_0A^{1/3})/a$, $x'=(r-r_0'A^{1/3})/a'$, and V_c is the Coulomb potential from a uniform charge of radius $r_cA^{1/3}$. The deuteron scattering was analyzed on the assumption of surface absorption only, that is, with $W=0$.

The He^3 energies involved in the present experiment range from about 16–19 MeV for Ca and from 12 to 17 MeV for Ti. Data were not available for the elastic scattering of He^3 ions of these energies, so the distorted-wave calculations for $Ti(d,He^3)$ were carried out by use of the optical potential found[9] to reproduce the scattering of 14-MeV He^3 from Fe^{54}. The scattering of 12-MeV He^3 from various nuclei including Ca^{40} and Sc^{45} has since been measured,[10] and preliminary analysis[11] has yielded a different set of optical-model parameters. These latter parameters were used in the analysis of $Ca(d,He^3)$, and both sets are given in Table II. Only volume absorption was considered, so that $W_D=0$. At the lower He^3 energies, both sets give very similar scattering in the forward hemisphere. At the higher energies encountered in the (d,He^3) experiments, their predictions begin to diverge. However, until scattering data at these energies are available, it is uncertain which set of parameters is to be preferred. Fortunately, both potentials lead to (d,He^3) cross sections with almost identical angular distributions in the

TABLE I. Optical-model parameters for Ti+d and Ca^{40}+d scattering at 21.5 MeV. Also given are the reaction cross sections σ_R predicted by the model.

A	V (MeV)	r_0 (F)	a (F)	W_D (MeV)	r_0' (F)	a' (F)	σ_R (mb)
40	100.5	1.053	0.968	29.0	1.520	0.429	1412
46	110.4	0.962	0.912	17.1	1.402	0.655	1577
47	111.0	0.955	0.920	19.0	1.447	0.599	1570
48	114.5	0.942	0.936	16.3	1.392	0.650	1604
49	110.0	0.974	0.912	18.4	1.439	0.599	1591
50	99.2	1.066	0.835	17.1	1.427	0.613	1591

[7] W. Tobocman, *Theory of Direct Nuclear Reactions* (Oxford University Press, New York, 1961); N. Austern, in *Fast Neutron Physics*, edited by J. B. Marion and J. L. Fowler (Interscience Publishers, Inc., New York, 1963), Vol. 2.

[8] R. H. Bassel, R. M. Drisko, and G. R. Satchler, Oak Ridge National Laboratory Report ORNL-3240, 1962 (unpublished); and G. R. Satchler (to be published).

[9] A. G. Blair and H. E. Wegner, Phys. Rev. **127**, 1233 (1962).

[10] J. L. Yntema and B. Zeidman (to be published).

[11] R. H. Bassel (private communication).

region of interest, and usually differ in magnitude by less than 20%.

Two further uncertainties are involved in the distorted-wave calculation of (d,He^3) reactions. The first is directly related to the absolute normalization of the predicted cross sections, and corresponds to the probability of finding the He^3 ion in the configuration $d+p$. We may write the differential cross section (mb/sr) in the form

$$d\sigma/d\omega = NS(lj)\sigma_{lj}(\theta),$$

where σ_{lj} is a "reduced" cross section calculated by the distorted-wave theory for pickup from an orbit with quantum numbers l and j, $S(lj)$ is the corresponding spectroscopic factor for the state,[12] and N is a normalization constant of order unity. Aside from physical constants, N includes the overlap for the dissociation of He^3 into $d+p$, and may be related to the asymptotic normalization of the He^3 internal wave function.[7,8] With the simplest zero-range assumption for the latter, the known dissociation energy leads to the estimate[8] $N\approx 1.2$. A more realistic wave function is expected to yield somewhat larger values. In terms of the constant Λ introduced in previous phenomenological analyses of these reactions,[12] $N=0.0081\ \Lambda$. These analyses yield values of Λ of the order of 200 for (d,t) reactions. This result again leads us to expect the value of N to be between 1 and 2. The present analysis determines N in two empirical ways, first by assuming the pickup in Ca^{40}(d,He^3) is from filled $1d_{3/2}(S=4)$ and $2s_{1/2}(S=2)$ shells, and secondly by assuming the ground states of the Ti isotopes contain just two ($S=2$) protons in the $1f_{7/2}$ orbit.

The second major uncertainty in the application of the simple distorted-wave theory concerns the physical significance of optical-model wave functions for complex particles such as deuterons and He^3 ions inside the nucleus. If it is assumed that little significance should be attached to the wave functions in this region, then the nuclear interior should be excluded from the stripping integrals by using a radial cutoff close to the nuclear surface. The comparison (Fig. 2) between theory and experiment for Ca^{40}(d,He^3)K^{39} clearly indicates a much better fit to the angular distributions when a cutoff is used. However, there is another aspect of this problem. In common with most calculations of this type, the so-called zero-range approximation has been used. More sophisticated calculations for this reaction have taken account of the finite size of the He^3 ion and the finite range of the $d-p$ interaction.[13] It is found that this leads to considerable damping of the contributions from the nuclear interior; its effects are very similar to those from using a cutoff in a zero-range calculation. For these reasons, the remainder of the analysis was carried out with the radial cutoff (or lower cutoff denoted L.C.O. in the figures).

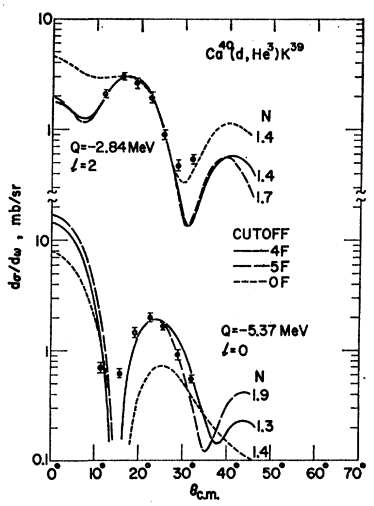

FIG. 2. Angular distribution for the Ca^{40}(d,He^3)K^{39} reactions. Both the ground-state transition ($Q=-2.84$ MeV) and the observed excited state ($Q=5.37$) are shown.

Two other minor uncertainties are concerned with the definition of the bound-state radial wave function for the proton before pickup. The present calculations compute this function for a proton moving in a potential well of Woods-Saxon shape and the Coulomb potential from a uniform charge of radius 1.25 $A^{1/3}$, with a binding energy equal to the separation energy of the proton. The surface diffuseness of the well is taken to be 0.65 F, while the choice of radius parameter is guided by optical-model analyses of proton scattering. The value $r_0=1.25$ F is usually taken for the latter,[14] although analyses of 40-MeV proton scattering indicate that $r_0=1.2$ is a better choice.[15] The smaller value leads to a predicted reduced cross section σ which has the same shape as that obtained with $r_0=1.25$ F but is 10–20% smaller, with a corresponding change in the empirically determined value of the normalization constant N. The other uncertainty arises from the spin-orbit coupling experienced by the proton in the bound state; the radial wave function is slightly different according to whether $j=l+\frac{1}{2}$ or $l-\frac{1}{2}$. The effect of a spin-orbit coupling 25 times the Thomas term is to increase (or decrease) σ by 10 to 20% when $j=l+\frac{1}{2}$ (or $l-\frac{1}{2}$). In other words, if values of σ calculated ignoring spin-orbit coupling are used, the normal-

TABLE II. Optical-model parameters for He^3 scattering.

Target	Energy (MeV)	V (MeV)	W (MeV)	r_0 (F)	a (F)
Fe^{54}	14	32	13	1.67	0.58
Ca^{40}	12	68	14	1.52	0.61
Sc^{45}	12	68	14	1.52	0.56
Sc^{45}	12	42	14	1.52	0.61

[12] M. H. Macfarlane and J. B. French, Rev. Mod. Phys. 32, 567, 1960.

[13] N. Austern, R. M. Drisko, E. C. Halbert, and G. R. Satchler, Phys. Rev. 133, B3 (1964).

[14] F. G. Perey, Phys. Rev. 131, 749, 1963.

[15] M. Fricke (private communication).

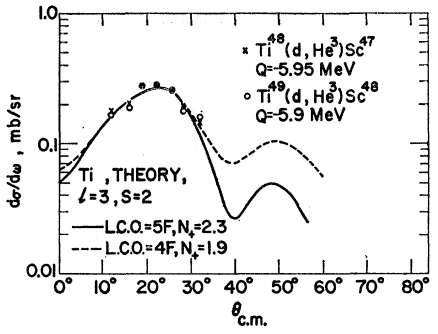

FIG. 3. Angular distributions of the ground-state transitions for the $Ti^{48}(d,He^3)Sc^{47}$ and $Ti^{49}(d,He^3)Sc^{48}$ reactions.

izing constant N becomes slightly j dependent. Again, the shape of the angular distribution is unaffected.

4. EXPERIMENTAL RESULTS AND INTERPRETATION

$Ca^{40}(d,He^3)K^{39}$

The spectrum of the $Ca^{40}(d,He^3)K^{39}$ reaction shows three strong peaks. The first two correspond to the ground-state transition and to a level in K^{39} at 2.58 $\pm$0.05 MeV. The third peak is assigned to the $O^{16}(d,He^3)N^{15}$ reaction. The angular distributions of the first two groups are shown in Fig. 2. The theoretical curves were obtained from distorted-wave zero-range calculations, as described in the previous section. The optical-model parameters are given in Tables I and II, while the proton bound states were computed with $r_0=1.25$. The effects of using a radial cutoff have already been noted; a cutoff at about 4 or 5 F gives reasonable agreement with experiment. (For comparison, the radius of the He^3 potential and the imaginary part of the deuteron potential is here 5.2 F, while the real part of the deuteron potential has a radius of 3.4 F.) If one assumes that the $2s_{1/2}$ shell is full ($S=2$) and the $d_{3/2}$ shell is full ($S=4$) and if one includes spin-orbit coupling in the calculation of the bound state of the proton, then the fits shown lead to the estimate $N\approx1.2\pm0.3$. Omitting this spin-orbit coupling *reduces* N from 1.6 to about 1.3, for the $d_{3/2}$ group. (Of course the $s_{1/2}$ bound state is unaffected.)

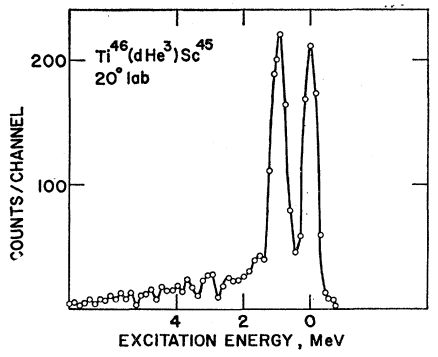

FIG. 4. Spectrum of the $Ti^{46}(d,He^3)Sc^{45}$ reaction at 20° lab.

Using $r_0=1.2$ *increases* N by about the same amount for both groups. These results suggest that the values

$$N_{\pm}\approx\begin{Bmatrix}1.6\pm0.3\\1.9\pm0.4\end{Bmatrix}\quad\text{if}\quad r_0=\begin{Bmatrix}1.25\\1.20\end{Bmatrix}$$

should be used for pickup with $j=l\pm\frac{1}{2}$ (if $l\neq0$) in zero-range calculations that neglect spin-orbit effects on the proton bound state, while for $l=0$ one should use $N_0=1.6$ (if $r_0=1.25$) or $N_0=1.9$ (if $r_0=1.20$). An over-all uncertainty of perhaps 20% should be associated with these numbers.

$Ti^{48,49}(d,He^3)$ Ground-State Groups

The angular distributions for the transitions to the ground states of Sc^{47} and Sc^{48} are shown in Fig. 3, which compares the experimental observations with the theoretical curves computed for Ti^{48} with radial cutoffs of 4 and 5 F. If the target nuclei are assumed to have exactly two protons in the $1f_{7/2}$ orbit ($S=2$), the fits shown correspond to normalization constants

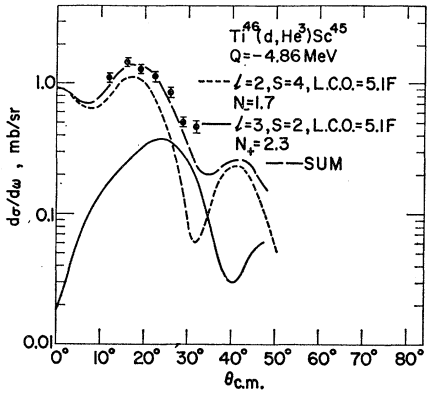

FIG. 5. Angular distribution for the $Ti^{46}(d,He^3)Sc^{45}$ reaction to the region near the ground state.

$N_{\pm}=1.9$ (cutoff at 4 F) and 2.3 (cutoff at 5 F) when $r_0=1.25$. These values are some 10% higher than would be expected from the Ca analysis, but the agreement is well within the uncertainties of the present analysis. These numbers are then used for the analysis of the remainder of the Ti data on the assumption that the corresponding values of N_- are 1.3 and 1.7, respectively.

$Ti^{46}(d,He^3)Sc^{45}$

The spectrum of the $Ti^{46}(d,He^3)Sc^{45}$ reaction is shown in Fig. 4. It shows two pronounced peaks, one at the Q value corresponding to the ground-state transition and one at an excitation energy of 0.93$\pm$0.05 MeV. The line shape is the same as the one for the $Ti^{48}(d,He^3)Sc^{47}$ transition in both cases. The angular distribution of the ground-state group is shown in Fig. 5. A comparison with the experimental results for the Ti^{48}-$(d,He^3)Sc^{47}$ ground-state transition (Fig. 3) shows that

the absolute cross section for the Ti^{46}(d,He^3)Sc^{45} is approximately 4 times as large and that the position of its maximum is shifted toward smaller angles. It appears therefore that the two ground-state transitions do not have the same value of l. The full curve represents the prediction for $l=3$ with $S=2$, while the dotted curve corresponds to $l=2$ and $S=4$. Both use a cutoff of 5 F. The sum of the two (dashed curve) is seen to be in good agreement with the experimental results. Since the spin and parity of Sc^{45} and Ti^{46} are known to be $7/2^-$ and 0^+, it follows that the ground-state transition has to correspond to the pickup of a $1f_{7/2}$ proton. The observed angular distribution then requires the presence of a $d_{3/2}$ hole state in Sc^{45} which, from the observed shape of the spectrum, has to be at an excitation energy less than 50 keV. The experimental results cannot be interpreted as the pickup of a $2p$ proton because, although this transition would be strong, its angular distribution peaks quite sharply at about 10°.

The angular distribution of the state near 0.92 MeV is shown in Fig. 6, the curves being calculated for

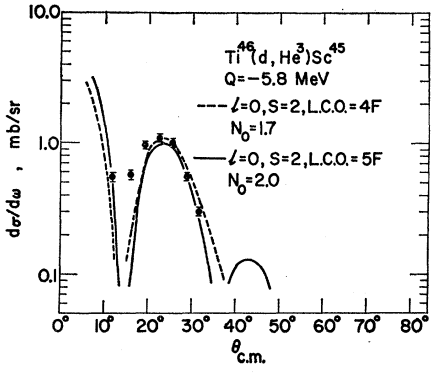

FIG. 6. Angular distribution for the Ti^{46}(d,He^3)Sc^{45} reaction to the 0.92-MeV state.

$l=0$, $S=2$, and cutoffs of 4 and 5 F. The good agreement indicates that this transition exhausts the $2s_{1/2}$ pickup strength.

Ti^{47}(d,He^3)Sc^{46}

The He^3 spectrum obtained at 20° is shown in Fig. 7. The peak near the ground state has its maximum pulse height at 0.135±0.04 MeV. It is a rather broad peak and certainly contains contributions from a number of states; the spectrum of levels in Sc^{46} is known to be rather dense even near the ground state. The shoulder visible at an excitation near 0.5 MeV has been clearly resolved at other angles and with thinner target materials. The center of that group is found at 0.595 ±0.065 MeV. The third group, which is rather clearly resolved and sharper than the ground-state group, has its center at 1.27±0.06 MeV. The angular distribution of the "ground-state" group, as well as that of the sum

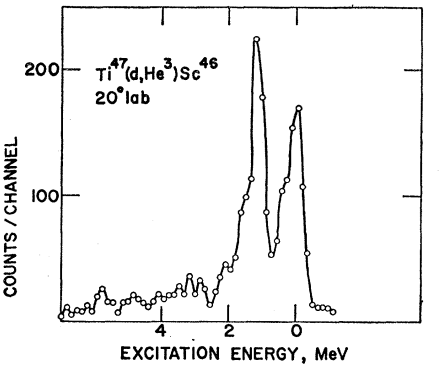

FIG. 7. Spectrum for the Ti^{47}(d,He^3)Sc^{46} reaction at 20° lab.

of the 0.6-MeV group and the "ground-state" group, is shown in Fig. 8. The theoretical curves are for $l=3$ pickup with $S=2$ and for $l=2$ with $S=3.2$. The sum of these two gives a reasonable fit to the experimental sum, but the "ground-state" group alone is very poorly fitted by $l=3$. Also shown is a mixture of $l=1$, $S=0.08$; $l=2$, $S=3.2$, and $l=3$, $S=1.0$. This mixture is in about as good agreement with experiment as is the sum neglecting the $l=1$ pickup with $l=3$, $S=2$.

The angular distribution of the group to the level(s) near 1.27 MeV is shown in Fig. 9, with the theoretical curve for $l=0$, $S=2$ with cutoff at 5 F. In this case the theoretical curve peaks at somewhat too large an angle. Also shown is the sum of the $l=0$ curve and the $l=2$, $S=1$ curve with the cutoff at 5 F.

Ti^{48}(d,He^3)Sc^{47}

The spectrum from the Ti^{48}(d,He^3)Sc^{47} reaction at 20° lab is shown in Fig. 10. The three groups correspond to the ground-state transition and the transitions to states at 0.80±0.05 and 1.44±0.08 MeV. The ground-

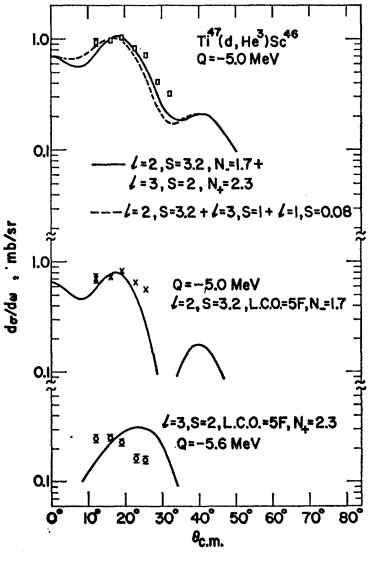

FIG. 8. Angular distributions of the He^3 groups from Ti^{47}(d,He^3)Sc^{46} reaction to the 0.135-MeV and 0.59-MeV states and of the sum of these groups.

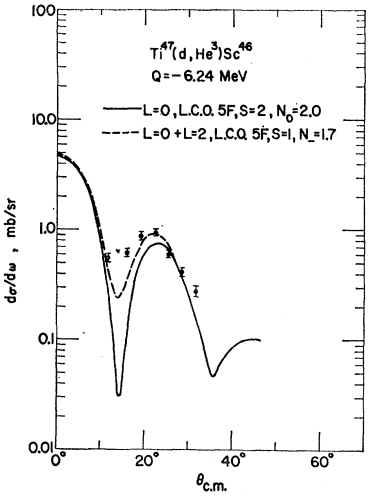

FIG. 9. Angular distribution for the $Ti^{47}(d,He^3)Sc^{46}$ reaction to the 1.27-MeV state in Sc^{46}.

state transition has already been discussed above. The angular distribution of the transition to the 800-keV level is shown in Fig. 11, with the predictions for $l=2$, $S(d_{3/2})=2.8$ and cutoffs of 4 and 5 F. The somewhat higher binding energy (12.24 MeV) of the proton associated with this group makes the theoretical angular distribution more sensitive to the exact value of the cutoff. Since the sharp cutoff is only a crude approximation, this sensitivity is somewhat unphysical. In view of this, the discrepancy between experiment and theory at the predicted minimum is not too serious, and the agreement at the peak makes it reasonable to assign a strength $S(d_{3/2})\approx 3$ to this level. It seems clear that this is principally a $d_{3/2}$ proton-hole state.

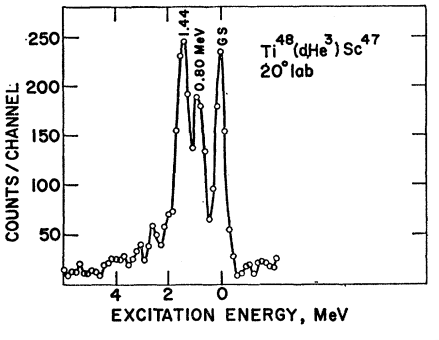

FIG. 10. Spectrum of the $Ti^{48}(d,He^3)Sc^{47}$ reaction at 20° lab.

The experimental angular distribution for the transition to the state at 1.42 MeV is shown in Fig. 12. The maximum in the angular distribution occurs at approximately the same angle as in the one for the ground-state transition. However, the maximum is much more pronounced than the one for $l=3$ angular distributions. The curves represent two distorted-wave Born approximation (DWBA) calculations for $l=0$, $S=2$—the solid curve with the cutoff at 4 F, the dashed one with the cutoff at 5 F. For either curve the strength $S=2$ gives a good fit to the secondary maximum. It is clear that the position of the first minimum is very sensitive to the choice of the cutoff radius. It appears that the experimental angular distribution would fit better with a narrower minimum. On the other hand, a possible admixture of an $l=2$ component in the experimental angular distribution would tend mainly to raise the experimental points between 12 and 20° but would have little effect on the remainder of the angular distribution. An admixture of $l=2$ with a strength of 1 would give the same result as the one

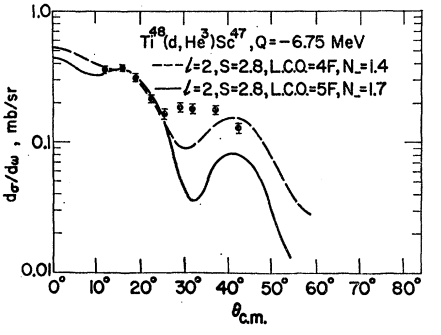

FIG. 11. Angular distribution for the $Ti^{48}(d,He^3)Sc^{47}$ reaction to the 0.80-MeV state of Sc^{47}.

shown for the 1.27-MeV group in Ti^{47}. Of course, it would be unwarranted to assume the existence of such an admixture merely from the comparison of the calculated curve and the experimental angular distributions.

$Ti^{49}(d,He^3)Sc^{48}$

The He^3 spectrum is shown in Fig. 13. The peak near the ground state appears to be within 40 keV of the ground-state Q value. Although the main strength of the $V^{51}(d,t)V^{50}$ reaction proceeds to the 4^+ state, there is no evidence that the main strength in the present reaction proceeds to a level above the ground state.

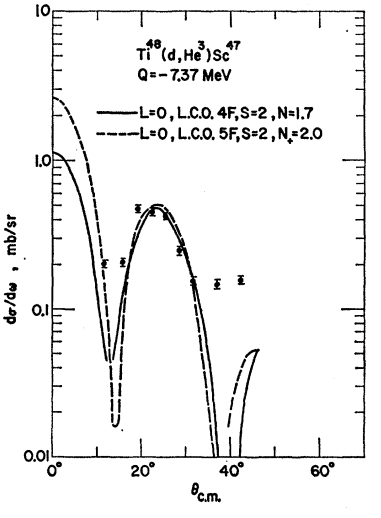

FIG. 12. Angular distribution for the $Ti^{48}(d,He^3)Sc^{47}$ reaction to the 1.42-MeV state of Sc^{47}.

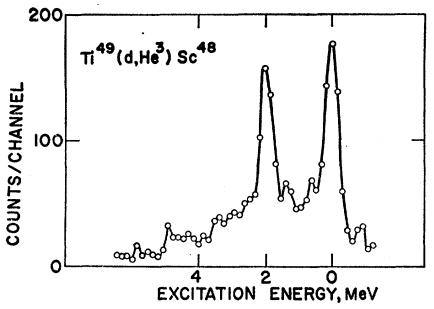

FIG. 13. Spectrum of the Ti^{49}(d,He^3)Sc^{48} reaction at 20° lab.

As discussed earlier, the angular distribution (Fig. 3) is fitted well with the calculated $l=3$ curve. The two weak states found at excitations of 0.77 and 1.40 MeV exhibit the behavior of $l=2$ transitions. They have about equal intensity and together they have more than 75% of the expected $d_{3/2}$ strength. The angular distribution of the 2.1-MeV state is shown in Fig. 14 together with curves for $l=0$ and $S=2$, with cutoffs at 4 and 5 F. From the comparison of the two curves, one may conclude that this state is an s-hole state with a strength close to 2.

Ti^{50}(d,He^3)Sc^{49}

The He^3 spectrum is shown in Fig. 15. Experiments with a thinner target show that only two states are

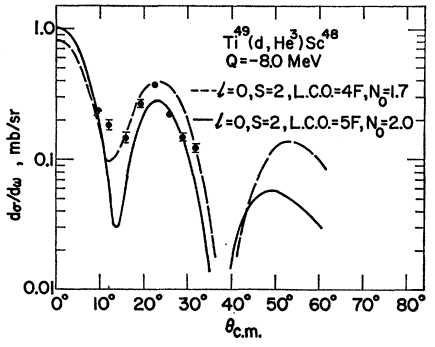

FIG. 14. Angular distribution for the Ti^{49}(d,He^3)Sc^{48} reaction to the state near 2.1 MeV.

observed: the ground state and a state near 2.40±0.15 MeV. The angular distribution of the ground-state group is shown in Fig. 16 together with the curve for $l=3$, $S=2$, and a cutoff at 5 F. The $l=3$ curve does not fit the data very well. Also shown for comparison is the $l=2$ curve with $S=1.2$ and the sum of the two curves.

The Q value of the Ti^{50}(d,He^3)Sc^{49} reaction is about the same as the one for the 800-keV transition in Ti^{48}(d,He^3)Sc^{47}. While it is quite likely that there are errors in the subtraction, these errors cannot give an apparent $l=2$ group with $S=1.2$. The maximum possible $l=2$ strength in the uncorrected data would be of the order of $S=0.6$. It seems rather unlikely that Sc^{49} would have a low-lying $p_{3/2}$ or $d_{3/2}$ hole state. The theoretical angular distribution is rather sensitive to the choice of cutoff radius; in particular, the choice of a smaller value of the lower cutoff (L.C.O.) would improve the fit to the data.

The angular distribution of the group found at an excitation of about 2.4 MeV is shown in Fig. 17, with the predicted curves for a cutoff at 5 F with $l=2$, $S(d_{3/2})=4$ and $l=0$, $S=1.3$. Their sum gives a good fit to the observed distribution. On the other hand, also shown for comparison are the predictions for $l=2$, $S(d_{3/2})=4$, when a cutoff at 6 F is used. Again, the strong binding (14.7 MeV) of this proton makes

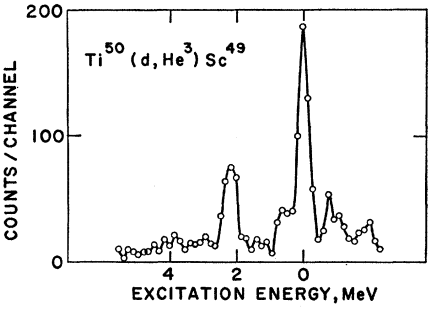

FIG. 15. Spectrum of the Ti^{50}(d,He^3)Sc^{49} reaction.

the predictions sensitive to the choice of cutoff. While 6 F is perhaps an unreasonably large value, it serves to illustrate the difficulty of determining l mixtures under these circumstances. In any case, it seems clear that this group has a considerable $l=2$ component whose strength approximately exhausts the $d_{3/2}$-hole strength.

5. DISCUSSION

The results are summarized in Table III. The two levels in K^{39} and the ground-state transition of Ti^{48}(d,He^3)Sc^{47} were used for normalization purposes. The strength used for the other transitions was obtained from the latter normalization. The *a priori* expectation was that one would observe three states in the Ti(d,He^3)Sc reactions on the even-even nuclei: the

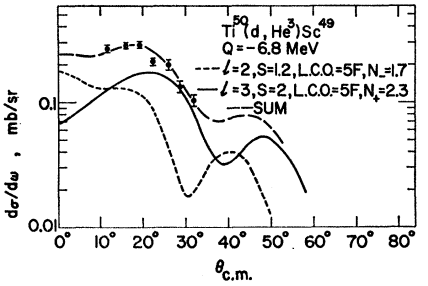

FIG. 16. Angular distribution for the ground-state transition of the Ti^{50}(d,He^3)Sc^{49} reaction.

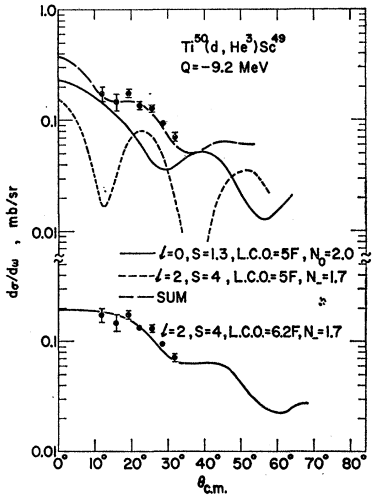

FIG. 17. Angular distribution of the $Ti^{50}(d,He^3)Sc^{49}$ reaction to the state at 2.4 MeV.

$l=3$ ground-state transition corresponding to the pickup of the $f_{7/2}$ proton, an excited state at least 2 MeV above the ground state (corresponding to the pickup of a $d_{3/2}$ proton), and the state corresponding to the pickup of an $S_{1/2}$ proton at least 4 MeV above the ground state. These expectations are based on the $d_{3/2}$—$s_{1/2}$ energy gap measured in both $Ca^{40}(d,He^3)K^{39}$ and $Ca^{40}(p,d)Ca^{39}$ and on the $f_{7/2}$—$d_{3/2}$ gap inferred from the difference observed when the Q value for nuclei with 22 neutrons is compared with the one for nuclei with 20 neutrons. Furthermore, the excitation energy at which the d- and s-hole states are found would be expected to shift somewhat as the number of $f_{7/2}$ neutrons in the nucleus is increased.

It is thus quite surprising to find the full strength of the $d_{3/2}$ hole state in Sc^{45} very close to the ground state. The lowest level previously reported in Sc^{45} is the 0.376-MeV level which has been observed in inelastic proton scattering and the $(n,n'\gamma)$ reaction. The conclusion that the d-hole state occurs at a very low excitation energy is derived from both the angular distribution and the cross section of the transition. The absolute cross section is approximately four times the value that would be obtained from the ground-state transition alone. The conclusion is further strengthened by the results obtained from the $Ti^{47}(d,He^3)Sc^{46}$ reaction in which the $d_{3/2}$ hole state is far enough from the ground state to permit its identification as an $l=2$ transition. The sum of the two lowest groups in the reaction on Ti^{47} reproduces both the angular distribution and the absolute cross section obtained on Ti^{46}. The fact that the d-hole state in Sc^{45} has not been observed in the (p,p') experiment may indicate that the excitation energy is lower than the upper limit of 50 keV deduced from the present experiment. Since the transition from the excited state to the ground state should be an $M2$ transition, it should have a rather long lifetime. The recent $Ca^{40}(p,\alpha)Sc^{43}$ results obtained by Holland and Lynch[16] indicate the existence of a low-lying positive-parity state in Sc^{43}.

TABLE III. Levels of the scandium isotopes.

Nucleus	Excitation energy of level (MeV)	l	Q (MeV)	S
Sc^{45}	0	3	−4.85	2 ($f_{7/2}$)
	0	+2		4 ($d_{3/2}$)
	0.92	0	−5.77	2
Sc^{46}	0.135	3	−5.10	2.0 ($f_{7/2}$)[a]
		+2		0.8 ($d_{3/2}$)[a]
	0.59	2	−5.56	3.2 ($d_{3/2}$)[a]
	1.27	0	−6.24	(2)
Sc^{47}	0	3	−5.95	2[b] ($f_{7/2}$)
	0.80	2	−6.75	2.8 ($d_{3/2}$)
	1.44	0	−7.39	(2)
Sc^{48}	0	3	−5.86	2[b] ($f_{7/2}$)
	0.77	2	−6.63	1.5
	1.40	2	−7.26	1.5
	2.1	0	−7.95	2
Sc^{49}	0	3	−6.8	2 ($f_{7/2}$)
		+2		1.2 ($d_{3/2}$)
		3[c]		2 ($f_{7/2}$)[c]
		+1[c]		0.2 ($p_{3/2}$)[c]
	2.4	2	−9.2	4 ($d_{3/2}$)
		2[d]		4 ($d_{3/2}$)[d]
		+0[d]		1.3[d]

[a] Possibly should be $l=3+2+1$.
[b] Normalized to make $S=2$.
[c] Alternative for 0 MeV.
[d] Alternative for 2.4 MeV.

When $f_{7/2}$ neutrons are added to the nucleus, the excitation energy of the $d_{3/2}$ hole state increases from 0.05 MeV for four $f_{7/2}$ neutrons to 0.2 MeV for five, 0.8 MeV for six, and 1.1 MeV for seven $f_{7/2}$ neutrons. This may be construed as the effect of the residual interaction of the $f_{7/2}$ neutrons with the $d_{3/2}$ protons. The excitation energy of the s-hole state similarly increases from 0.92 MeV for four $f_{7/2}$ neutrons to 1.27 MeV for five, 1.44 MeV for six, 2.1 MeV for seven, and 2.5 MeV for eight neutrons.

In the $Ti^{47}(d,He^3)Sc^{46}$ reaction, it is not possible to ascertain whether or not the ground state is observed. There is, however, a strong indication that the peak near 0.135 MeV is a transition to a $d_{3/2}$-hole state.

ACKNOWLEDGMENTS

The technical assistance of W. J. O'Neill and the cooperation of the Argonne cyclotron group are gratefully acknowledged. We are also indebted to R. M. Drisko and R. H. Bassel for helpful discussions and for making the DWBA calculations possible.

[16] F. J. Lynch and R. E. Holland (private communication).